CHAPTER IV
SYNTHESES OF POROUS CLAY HETEROSTRUCTURES FROM LOCAL CLAY MINERALS

4.1 ABSTRACT

Porous clay heterostructures (PCH) derived from montmorillonite and bentonite were obtained by the surfactant-directed assembly of mesostructured silica within clay layers. X-ray diffraction (XRD), thermalgravimetric analysis (TGA), N_2 adsorption-desorption, scanning electron microscopy (SEM) and transmission electron microscope (TEM) were used to characterize the montmorillonite-PCH (denoted PMH) and bentonite-PCH (denoted PBH). There are two different methods, calcination or solvent extraction, for surfactant removal from the pores which are investigated on the porous properties. By both methods, PMH and PBH exhibited a BET surface area in the range 400-700 m^2/g and the corresponding pore volumes were in range 0.3-0.5 cm^3/g. The framework pore sizes were in the supermicropore to small mesopore range (1.7-3.9 nm).

keywords: porous clay heterostructure, montmorillonite, bentonite.

4.2 INTRODUCTION

Since the surfactant used as templates for synthesizing M41S can be intercalated into the interlayer galleries of clays, templated synthesis could be applied for the synthesis of highly porous clays. In 1995 the discovery of a new porous materials known as porous clay heterostructure (PCH) has been reported [1]. The approach is the combination of the conventional pillaring process and the liquid crystal templating mechanism, affording materials with uniform pore diameters in the supermicropore to small mesopore range (1.5 − 3.0 nm), with high specific surface areas and high thermal stability [2].

These materials were prepared by the surfactant-directed assembly of mesostructured silica within the two-dimensional galleries 2:1 mica type layered

silicate, such as in fluorohectorite [1,3], synthetic saponite [2, 4-6], montmorillonite [5-8] and vermiculite [9].

In the first step of preparation of PCH, the clay is expanded by exchange with a cationic surfactant as a template to allow an easier access to the interlayer region. A neutral amine as co-template is then intercalated. Subsequently, a silica source is formed in situ by polymerizing around templates. By either calcination or solvent extraction, the templates are removed from the solid and are replaced by protons.

The advantages of this approach are that the pore volume can be controlled by the volume of the template constituents and the pore size is controlled by the size of the surfactant micelles. The effect of the chain length of the quaternary ammonium surfactants on the pore size was studied [10]. The pore size was directly proportional to the chain length of surfactants. This indicates a molecular templating mechanism, similar to that observed in the synthesis of MCM-41. Moreover, the different chain length of neutral amine was used in the synthesis [11]. The samples were obtained, having not much different in the surface areas and pore volume. In addition, the different proportion of neutral amine and silica source (TEOS) was observed. It can be noticed that the increase in the amount of the neutral amine increased the micropore volume and decreased the mesopore volume.

In this research work, The synthesis of porous clay heterostructures from the two different clay minerals (commercialized-montmorillonite and local-bentonite) have been focused and studied the effect of surfactant chain length on the pore size, pore volume and specific surface areas. Moreover, the different methods of surfactant removal have also compared the surface areas and the pore characteristic. Continuous work will focus on the blending of PCH with polypropylene, producing a nanocomposites and study the gas barrier and thermal properties of these nanocomposites.

4.3 EXPERIMENTAL

Materials

Two different clays have been used in this study for the synthesis of porous clay heterostructures (PCH). Montmorillonite (MMT) was obtained from Kunimine Industries Co., Ltd. and bentonite (BN) was obtained from Thai Nippon Chemical Industry Co., Ltd. which have a cation exchange capacity (CEC) of 115 and 52 mmol/100g clay, respectively.

Alkyltrimethylammonium $[C_nH_{2n+1}N^+(CH_3)_3]$ bromide (n = 16) was supplied by A.C.S. Xenon Limited Partnership (Fluka) and chloride (n = 12, 18) were obtained from Kao Industrial (Thailand) Ltd. Tetraehtyl orthosilicate (TEOS) was supplied by A.C.S. Xenon Limited Partnership (Fluka) and dodecylamine was supplied by S.M. Chemical Supplies Co., Ltd. (Aldrich).

Synthesis of PCH

3 g of clay was added to 50 mL of alkyltrimethylammonium cation and stirred at 50°C for 24 h. After the exchange reaction the solid was filtrated out, washed with a mixture of methanol and water, and air-dried. The obtained organoclays are named MMT-C_n and BN-C_n (where n is the no. of carbon on the main alkyl chain) for organo-montmorillonite and organo-bentonite. Organoclay was stirred in dodecylamine for 30 min at room temperature after which TEOS was added. The resulting suspension was stirred for further 4 h at room temperature. The molar ratio of organoclay : dodecylamine : TEOS was 1 : 20 : 150. After reaction time the solid was separated from solution again by filtration and air-dried overnight at room temperature to form the as-synthesized PCH. The surfactant was removed from the as-synthesized PCH either by calcination or by solvent extraction. For calcination, the as-synthesized PCH was calcined at 600°C for 5 h using a temperature ramp rate of 1°C/min. The obtained PCH are named cal-PMH-C_n and cal-PBH-C_n for montmorillonite-PCH and bentonite-PCH, respectively. In the case of extraction, the surfactant was extracted from the as-synthesized PCH using HCl/methanol solution. Typically, 1 g of as-synthesized PCH material has been

added to 45 mL of methanol and 5 mL of HCl and refluxed for 2 h. The solid was subsequently filtrated out and washed with a mixture of methanol and water and air-dried at room temperature overnight. The obtained PCH are named ext-PMH-C_n and ext-PBH-C_n for montmorillonite-PCH and bentonite-PCH, respectively.

Physical Measurements

Powder X-ray diffraction patterns were measured on a Rigaku Model Dmax 2002 diffractrometer with Ni-filtered Cu K_α radiation operated at 40 kV and 30 mA. The powder samples were observed on the 2θ range of 1.2-20 degree with scan speed 2 degree/min and scan step 0.01 degree.

N_2 adsorption-desorption isotherms were obtained at -196°C on a Sorptomatic 1990 series ThermoFinnigan. Samples were degassed at 200°C during 12 h in a vacuum furnace prior to analysis. Surface areas were calculated using the BET equation. The pore size distributions were constructed based on Barrett, Joyner and Halenda (BJH) method using the adsorption branch of the nitrogen isotherm.

TG-DTA curves were collected on a Perkin-Elmer Pyris Diamond TG/DTA instrument. The sample was loaded on the platinum pan and heated from 30°C to 900°C at a heating rate of 10°C/min under N_2 flow.

Scanning electron microscopy was performed on JSM-6400 Model. The specimens were coated with gold under vacuum.

Transmission electron microscopy was performed on JEOL JEM-2100 electron mocroscope and an accelerating voltage of 160 kV. TEM samples were prepared by embedding the powder in resin and sectioning on a ultramicrotome. The thin sections were supported on copper grids.

4.4 RESULTS AND DISCUSSION

Characterization of Montmorillonite and Bentonite and Organo-Montmorillonite and Bentonite

Montmorillonite (MMT) and bentonite (BN) have a cation exchange capacity (CEC) of 115 and 52 mmol/100g clay, respectively. Both corresponding XRD patterns show the presence of the (001) reflection peak. As shown in Fig. 4.1 and 4.2, the basal spacing of MMT is 1.27 nm (Fig. 4.1(b)). After calcination at 600°C, the d_{001} value decrease to 0.97 nm (Fig. 4.1(a)) which can be approximately considered as the thickness of a single MMT layer. For bentonite, the basal spacing is 1.53 nm (Fig. 4.2(b)) and the thickness of each layer is 0.98 nm (Fig. 4.2(a)).
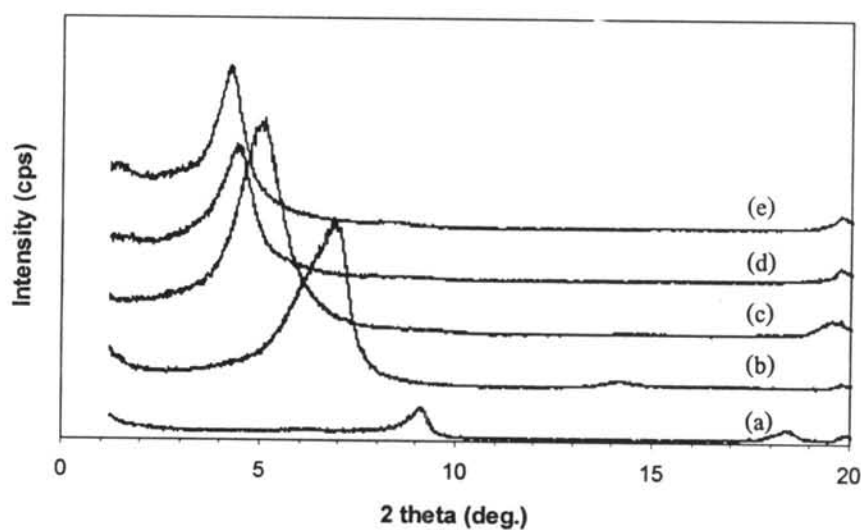
Figure 4.1 The XRD pattern of montmorillonite: (a) MMT calcined at 600°C (b) MMT (c) MMT-C$_{12}$ (d) MMT-C$_{16}$ (e) MMT-C$_{18}$.
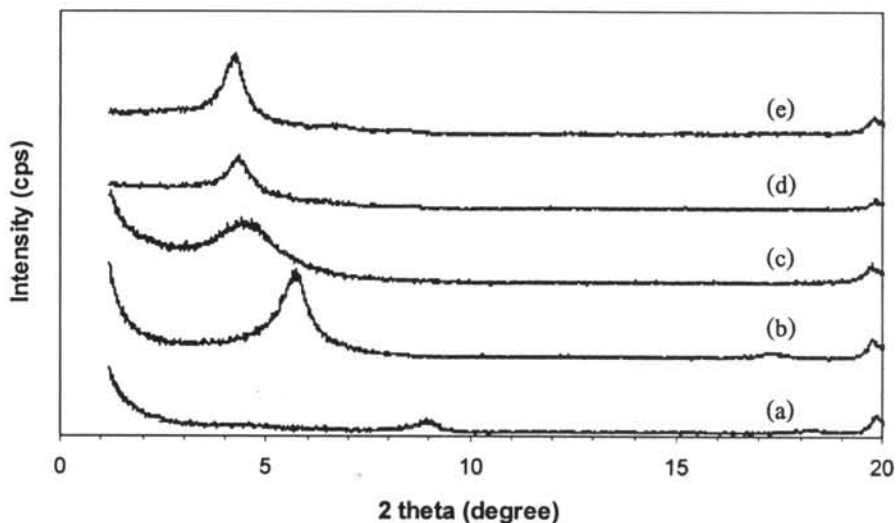
Figure 4.2 The XRD pattern of bentonite: (a) BN calcined at 600°C (b) BN (c) BN-C_{12} (d) BN-C_{16} (e) BN-C_{18}.

When two different clays was treated with alkyltrimethylammonium cations, the peak of starting clays disappeared and a new peak appeared at small angle (2θ). From Fig. 4.1(c)-(e) and Fig. 4.2(c)-(e), the (001) reflection peaks were shifted to the smaller angle and the increased d_{001} values, corresponding to Bragg's law. As a result of alkyltrimethylammonium cations readily intercalate in the interlayer and increase the distance between layers. Moreover, the differrent alkyl chain length (n) shows the differrent d_{001} value which is illustrated in Table 4.1

As can be seen from Table 4.1, the d_{001} value of MMT increase from 1.27 nm to 1.75, 1.98 and 2.08 nm as the alkyl chain length (n) increase to 12, 16 and 18, respectively. Thus, the longer alkyl chain length can be more expanded the interlayer distance. In the case of bentonite, the d_{001} increase from 1.53 nm to 1.97, 2.02 and 2.05 nm which has the same tendency as MMT.

Formation of Motmorillonite-PCH and Bentonite-PCH

The synthesis of PCH can be divided into 2 steps; in the first step the gallery sodium ions in the clay host are exchanged for surfactant ions which are alkyltrimethylammonium cations. The clay layers is expanded, which facilitates the accessibility of co-surfactant (neutral amine) and silica source (TEOS) in the second

step. The intercalation of the surfactant, co-surfactant and silica source in the clay interlayer region gives rise to a rod-like micellar structure as in "the liquid crystal template" of the hexagonol MCM-41.

Table 4.1 Comparison of the basal spacing of the starting clay and organoclay of montmorillonite and bentonite

Sample	2θ	d-value (nm)	Sample	2θ	d-value (nm)
MMT cal600*	9.110	0.97	BN cal600*	9.00	0.98
MMT	6.940	1.27	BN	5.760	1.53
MMT-C_{12}	5.050	1.75	BN-C_{12}	4.480	1.97
MMT-C_{16}	4.450	1.98	BN-C_{16}	4.380	2.02
MMT-C_{18}	4.240	2.08	BN-C_{18}	4.300	2.05

* The virgin montmorillonite and virgin bentonite were calcined at 600°C.

Table 4.2 Comparison of the basal spacing of the as-synthesized PCH of montmorillonite and bentonite

Sample	2θ	d-value (nm)	Sample	2θ	d-value (nm)
PMH-C_{12}	3.400	2.60	PBH-C_{12}	1.980	4.46
PMH-C_{16}	2.380	3.71	PBH-C_{16}	2.350	3.76
PMH-C_{18}	3.300	2.68	PBH-C_{18}	2.200	4.01

After the co-intercalation of dodecylamine and TEOS, the basal spacing becomes larger due to the intercalation of dodecylamine and TEOS and occuring the interlayer hydrolysis condensation polymerization of TEOS. The d_{001} values of as-synthesized PMH and PBH are also given in Table 4.2. The corresponding XRD patterns are shown in Fig. 4.3 and 4.4. The d_{001} of as-synthesized PMH increase to

2.60, 3.71 and 2.68 nm for PMH-C_{12}, PMH-C_{16} and PMH-C_{18}, respectively. In addition, the d_{001} values of as-synthesized PBH-C_{12}, PBH-C_{16} and PBH-C_{18} are 4.46, 3.76 and 4.01 nm, respectively.
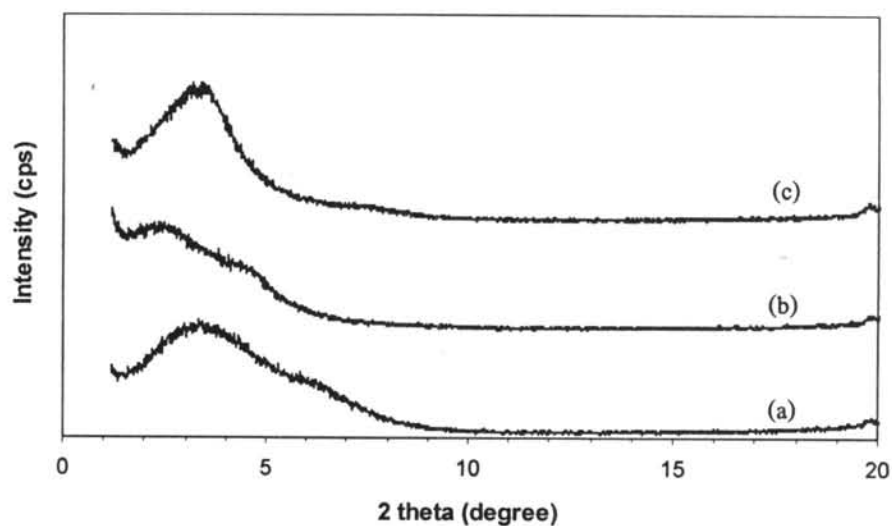
**Figure 4.3** The XRD pattern of as-synthesized PMH: (a) PMH-C_{12} (b) PMH-C_{16} (c) PMH-C_{18}.
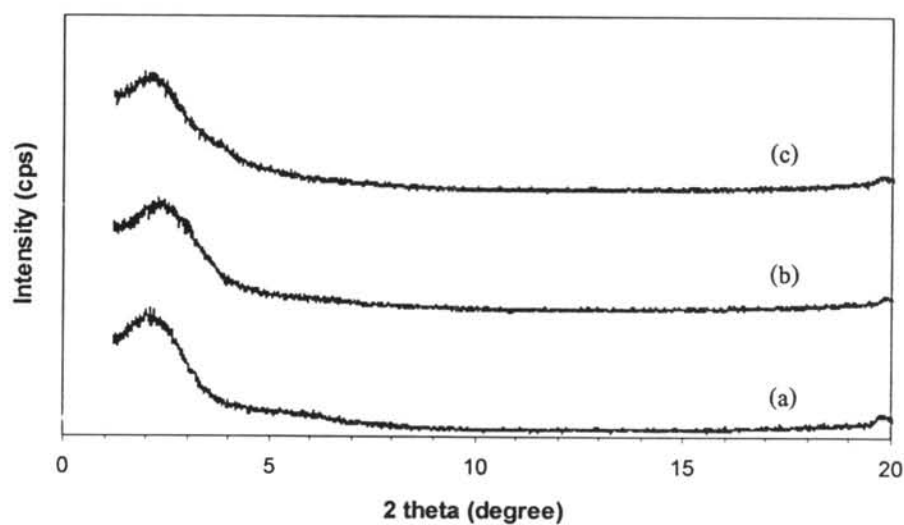
**Figure 4.4** The XRD pattern of as-synthesized PBH: (a) PBH-C_{12} (b) PBH-C_{16} (c) PBH-C_{18}.

Thermal Analysis of As-synthesized PCH

The thermogravimetric analysis curves of as-synthesized PMH and PBH were shown in Fig. 4.5 and 4.6. The as-synthesized PMH and PBH show three stages of weight loss. The first stage below 100°C is belong to elimination of physical adsorbed water which revealed about <5% weight loss. The second stage in temperature range of 150-350°C is attributed to the elimination and decomposition of neutral amine and surfactant. The third stage in temperature range of 350-600°C gradually decreasing is more likely to the removal of residue organic species. The loss of weight in temperature range 150-600°C increases with the carbon chain length (n) of the surfactant. The weight loss of as-synthesized PMH are about 27% for PMH-C_{12}, 31% for PMH-C_{16} and 32% for PMH-C_{18}. As-synthesized PBH also has the same tendency, the weight loss are about 27% for PBH-C_{12}, 29% for PBH-C_{16}, 30% for PBH-C_{18}.
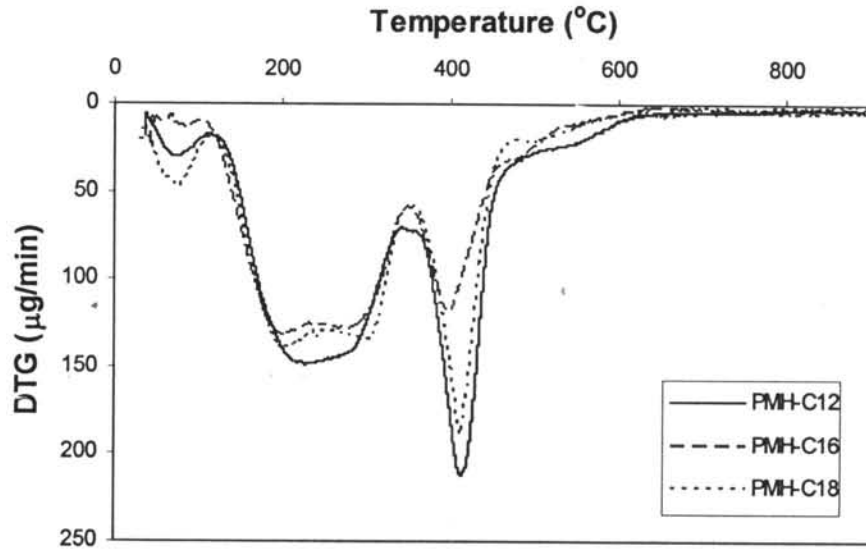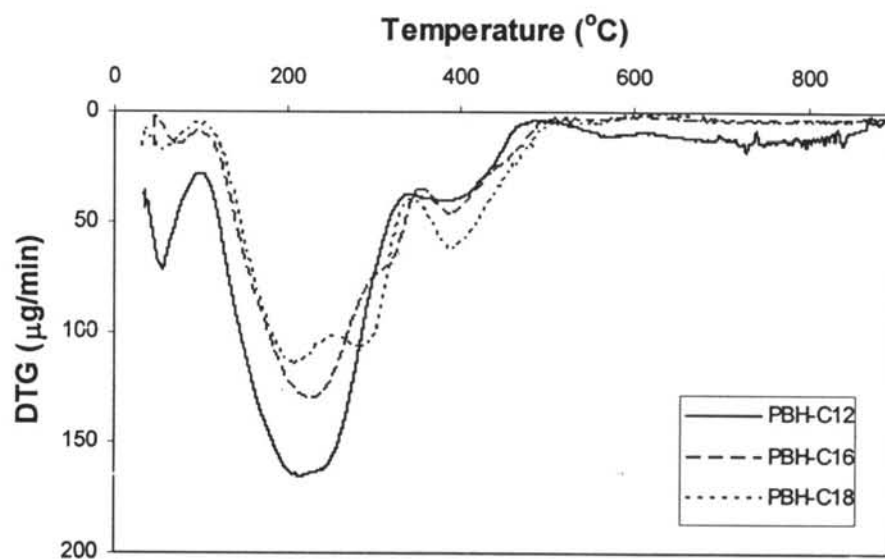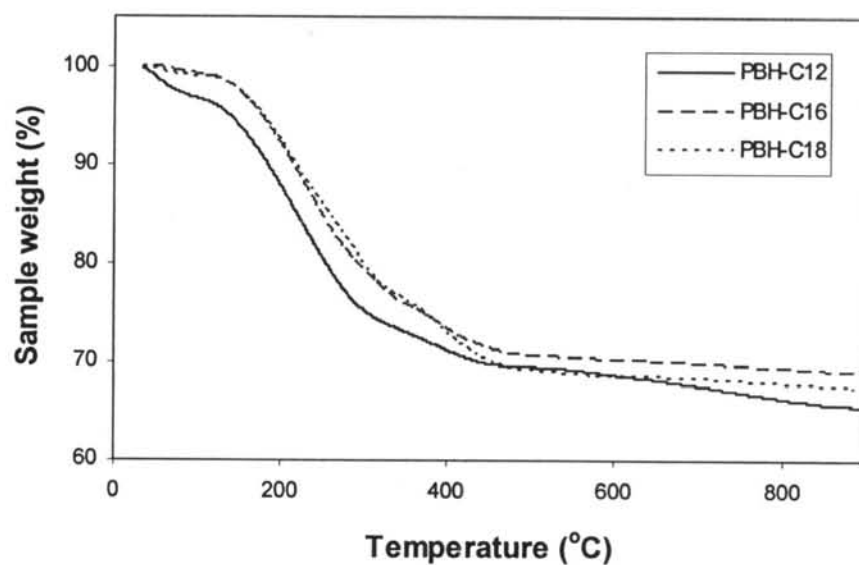
(A)
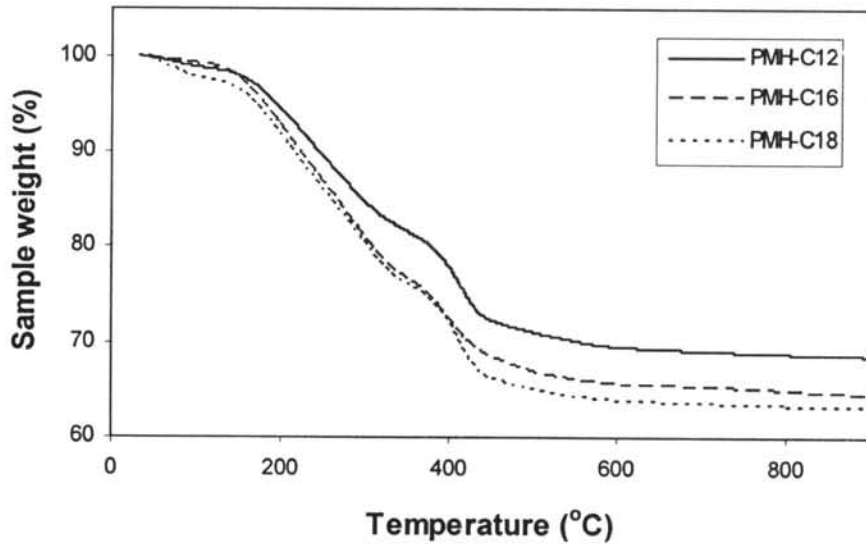
(B)

Figure 4.5 TG-DTA curves of the as-synthesized PMH (A) differential weight loss curves (DTG) (B) weight losses of the uncalcined samples when heated up to 900°C.

(A)

(B)

Figure 4.6 TG-DTA curves of the as-synthesized PBH (A) differential weight loss curves (DTG) (B) weight losses of the uncalcined samples when heated up to 900°C.

Pore Characterization

Montmorillonite (MMT) and bentonite (BN) show a layered or platelike structure in SEM images (Fig. 4.7(A)). The BET surface areas of MMT and BN are 42.07 and 58.52 m^2/g, respectively. This can indicate that MMT and BN are a non-porous solid. The SEM image of porous clay heterostructure after calcination (Fig. 4.7(B)) shows a roughness and a porosity on the surface of clay layers comparing to original montmorillonite. In the TEM image provided in Figure 4.8, the clay layers are discernible as solid dark lines and the pores appear in lighter contrast between the layers. The framework pore orientation is not persistent, however, indicating a significant degree of disorder within the gallery. A disorder wormhole-like pore structure in the *ab* plane is suggested by the changes in contrast levels between the layers.
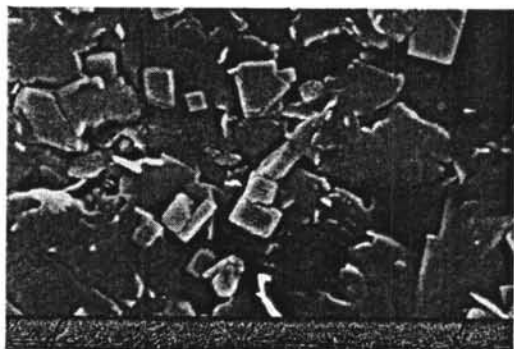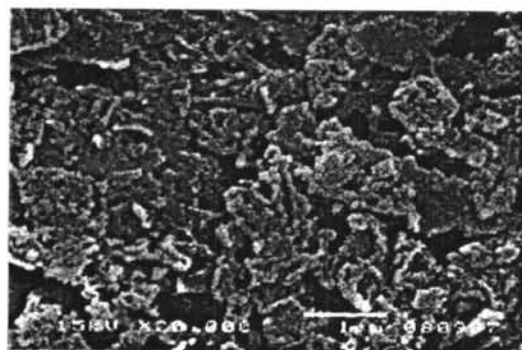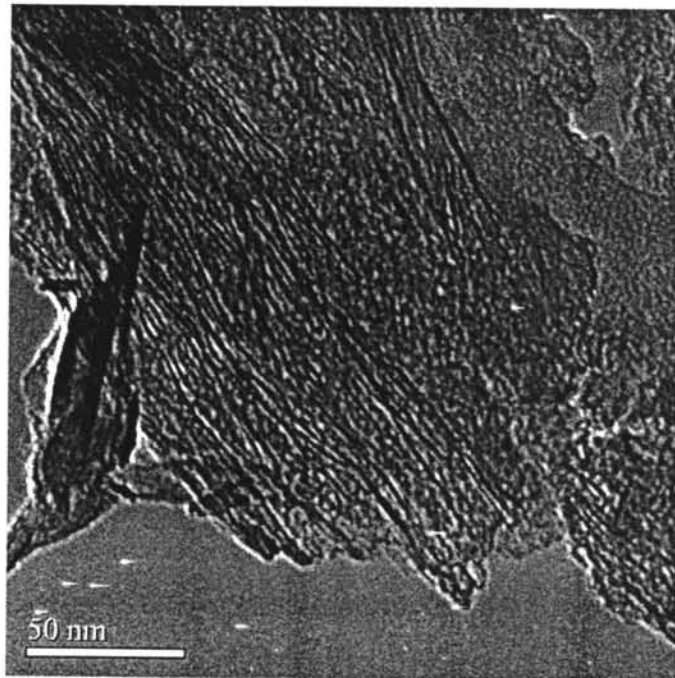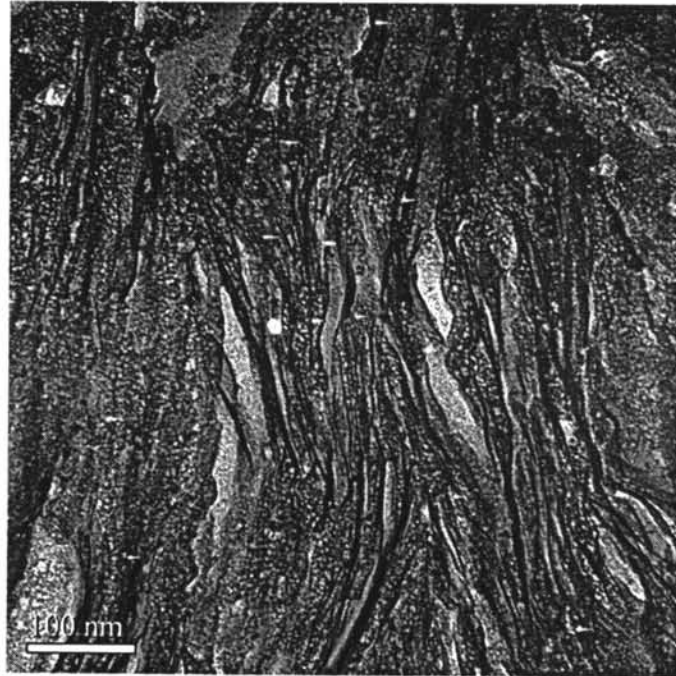

(A)   (B)

Figure 4.7 The SEM images: (A) montmorillonite (B) porous clay heterostructure.

**Figure 4.8** The TEM images of thin-sectioned porous clay heterostructure.

By calcination, the surfactants (templates) are removed from the as-synthesized PMH and PBH. The N_2 adsorption-desorption isotherm of PMH and PBH after calcination are shown in Fig. 4.9, the parameters of which are listed in Table 4.3. The isotherms of PMH and PBH are similar. The shape of isotherms for both sample has a hysteresis loop which belong to a type IV BET isotherm according to the BDDT classification. The near-linear uptake of nitrogen in the knee region corresponding to the partial pressure range 0.05-0.3 is indicative of a supermicropore to small mesopore structure in the supermicropore to small mesopore region. Furthermore, they exhibit a type B hysteresis loop, indicating the presence of the slit-shaped pores in PMH and PBH [12]. The BET specific surface areas of the calcined PMH and PBH were in the range 500-700 m^2/g and the corresponding pore volumes were in range 0.4-0.5 cm^3/g. The pore sizes which analyzed by BJH method were 1.7-3.8 nm.

An alternative method to remove the surfactants is solvent extraction. The N_2 adsorption-desorption isotherm of PMH and PBH after solvent extraction are shown in Fig. 4.10. The porosity characteristics are summerized in Table 4.4. The shapes of the N_2 adroption-desorption isotherms of both calcined and extracted-PCH are very similar which belong to a type IV BET isotherm and show a type B hysteresis loop. The BET specific surface areas of the extracted PMH and PBH were in the range 400-600 m^2/g and the pore volumes were in range 0.3-0.5 cm^3/g. The pore sizes were 1.7-3.8 nm. It can be noted that both specific surface area of calcined and extracted PCH tend to increase with increasing the alkyl chain length of surfactant.

It has been shown that in some cases, calcination can result in slight structural collapses and give lower porosities, due to the increase in local heating effects that are built up in the materials [6]. This is also evidenced by the larger hysteresis appearing in the isotherm desorption branch of calcined PMH and PBH compared to extracted one. In addition, calcination promotes condensation of unreacted silanol groups, and many surface groups are lost at typical calcinations temperatures [13] because the framework is dehydroxylated and crosslinking of the silica channels to the clay layers occurs. By solvent extraction the surfactant removal promotes the polycondensation of siloxane oligomers to stable polysiloxane, which forms a three-dimensional network of Si-O-Si bonds. The development of the siloxane network

results in the additional formation of micropores among the Si-O-Si bonds. On the other hand, the calcination of PMH and PBH results in the condensation/dehydration of the siloxane compound to form silica particles in the gallery, from which the narrow spaces among the polysiloxane network dissappear while relatively wide spaces form among the calcined particles. Therefore, the extracted PCH have narrower pores than calcined products [9].

The amount of residual surfactant remaining on the PMH and PBH structure was determined by TG-DTA as can be seen in Fig. 4.11 and 4.12. For the extraction, the weight loss in temperature range 300-600°C of the extracted PMH and PBH are about 8-12%. On the other hand, the residual surfactants are less than 3% for calcination which are listed in table 4.5. In this work, the calcination method is preferable for the surfactant removal, due to its easy method and no needs to use a lot of solvent.
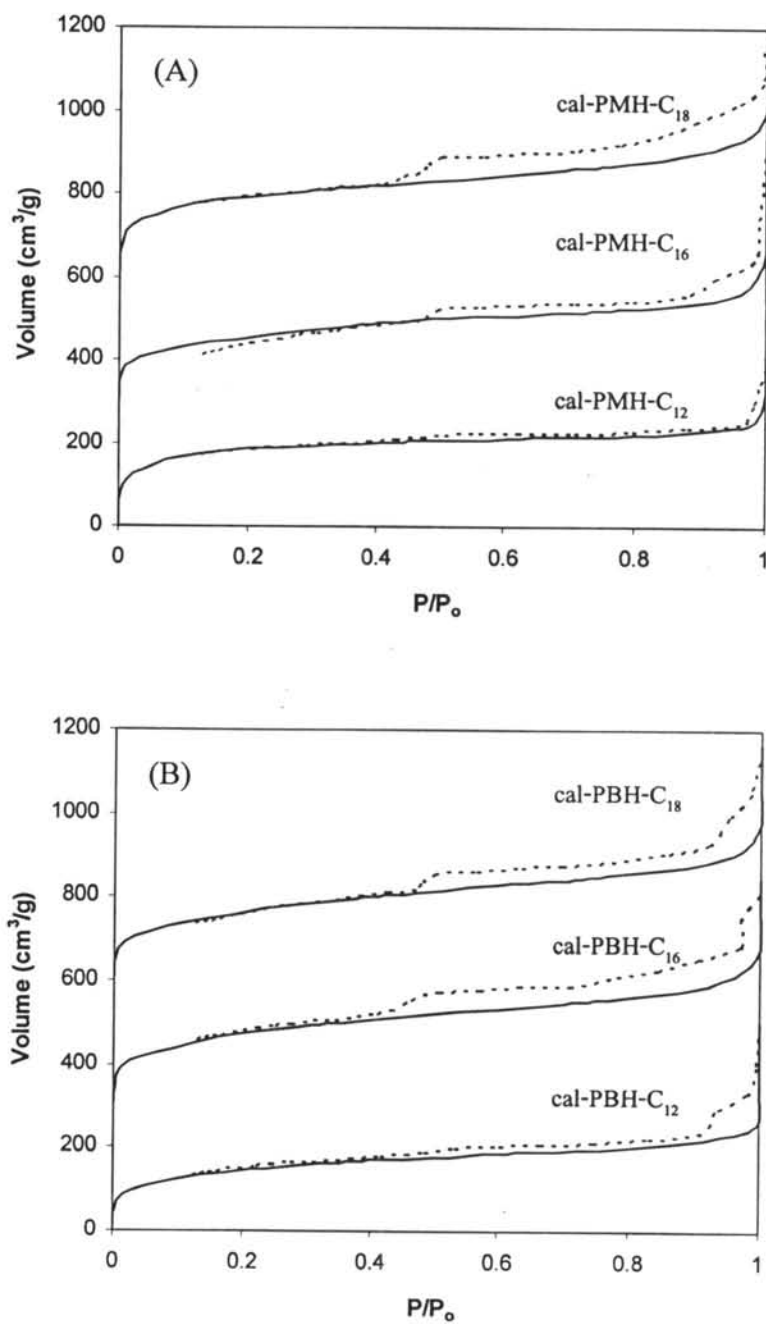
Figure 4.9 The N_2 adroption-desorption isotherm of calcined samples (A) mont-morillonite-PCH (B) bentonite-PCH. Solid line and dash line represent adsorption and desorption, respectively.
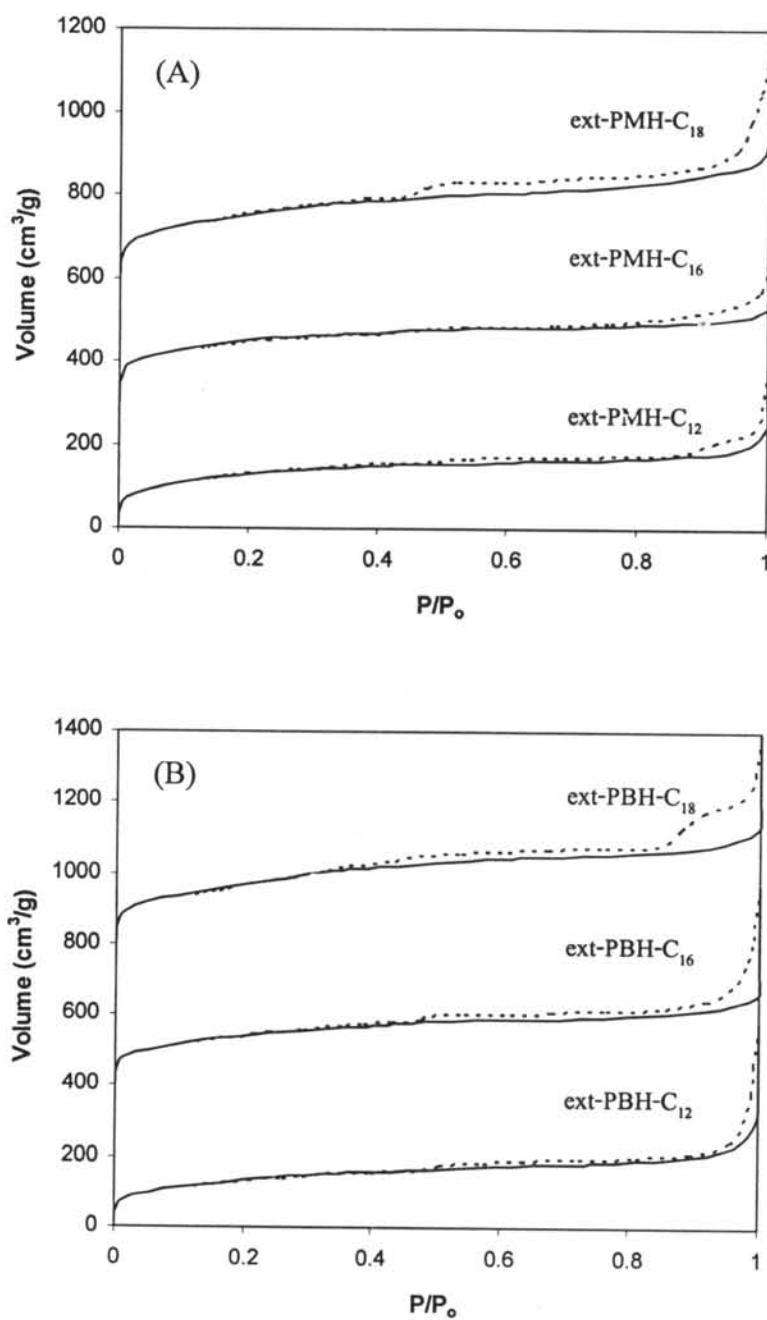
Figure 4.10 The N_2 adroption-desorption isotherm of extracted samples (A) mont-morillonite-PCH (B) bentonite-PCH. Solid line and dash line represent adsorption and desorption, respectively.

**Table 4.3** The porosity characteristics of calcined PMH and calcined PBH

Sample	specific surface areas (m^2/g)	Pore specific volume (cm^3/g)	Pore diameter (nm)
cal-PMH-C$_{12}$	606.57	0.45	1.75
cal-PMH-C$_{16}$	689.38	0.52	3.88
cal-PMH-C$_{18}$	746.80	0.51	3.78
cal-PBH-C$_{12}$	652.90	0.40	2.36
cal-PBH-C$_{16}$	731.57	0.49	3.71
cal-PBH-C$_{18}$	729.80	0.47	3.80

Table 4.4 The porosity characteristics of extracted PMH and extracted PBH

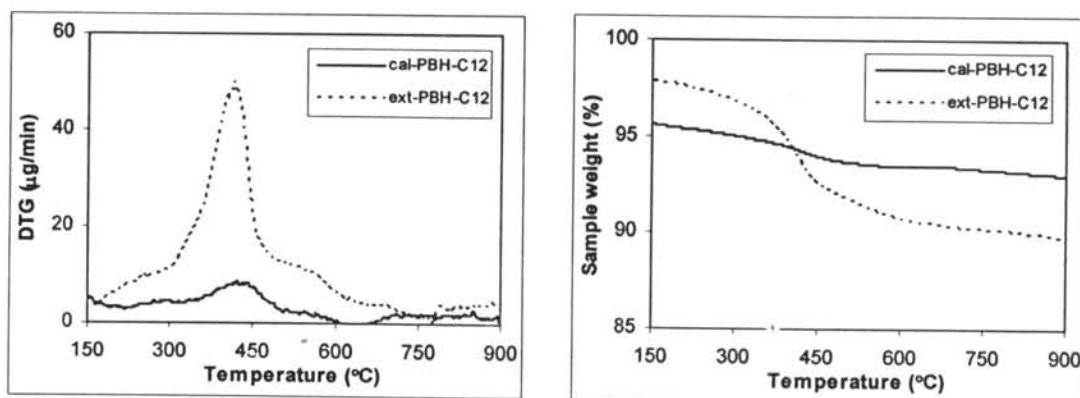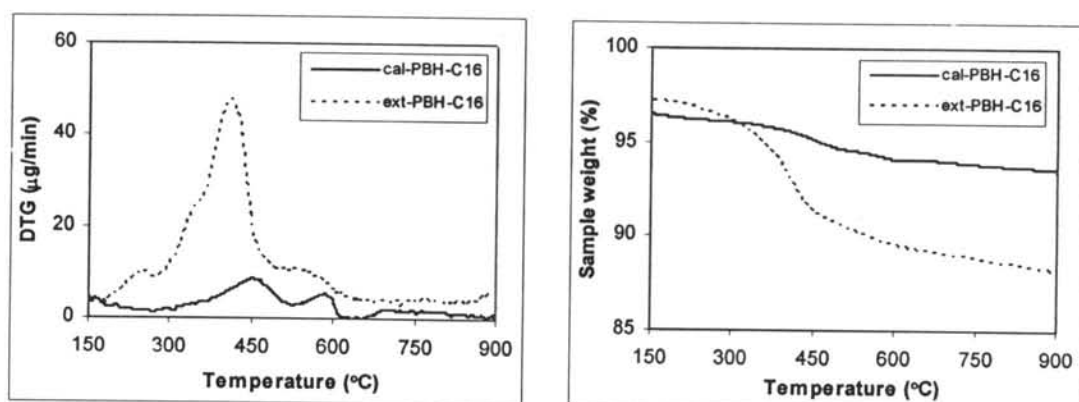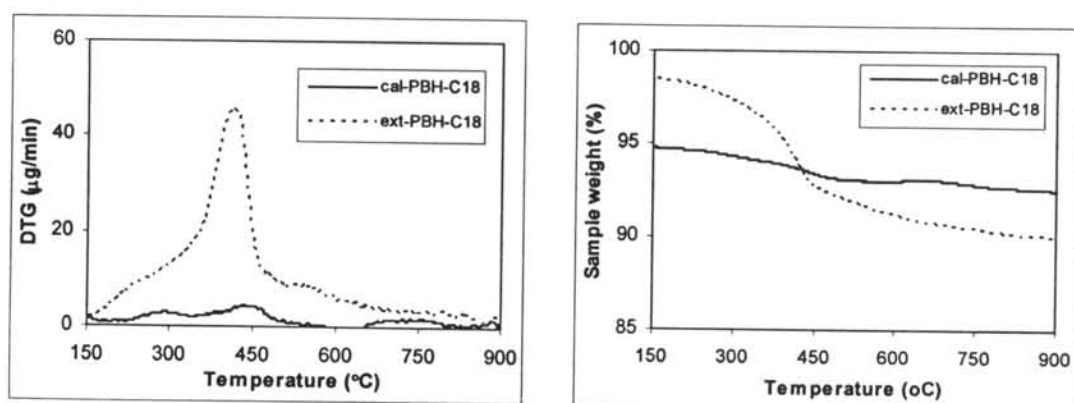| Sample	specific surface areas (m^2/g)	Pore specific volume (cm^3/g)	Pore diameter (nm)
ext-PMH-C$_{12}$	439.58	0.38	2.00
ext-PMH-C$_{16}$	540.85	0.31	1.74
ext-PMH-C$_{18}$	576.75	0.45	3.74
ext-PBH-C$_{12}$	476.23	0.47	1.81
ext-PBH-C$_{16}$	500.76	0.39	3.82
ext-PBH-C$_{18}$	629.99	0.64	1.85
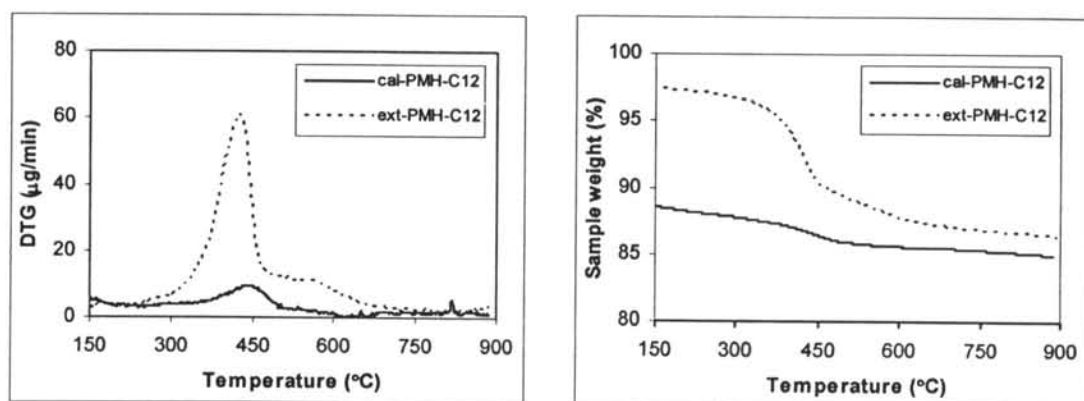
(A)
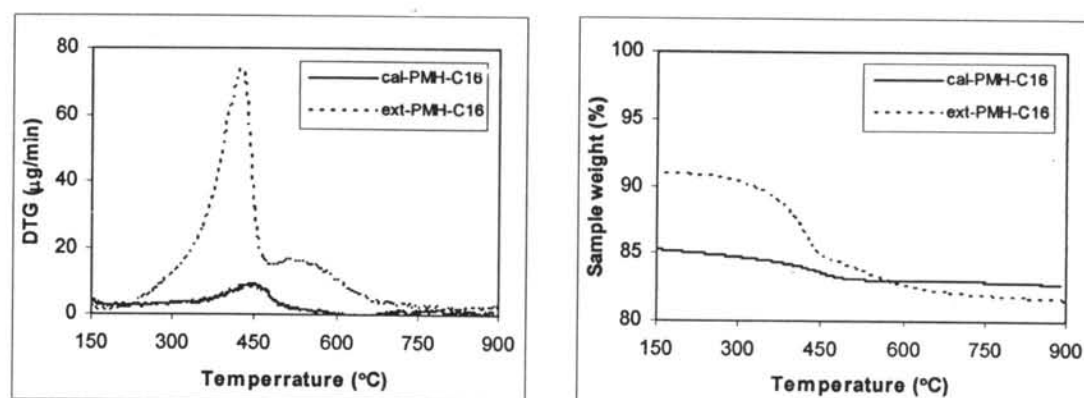
(B)
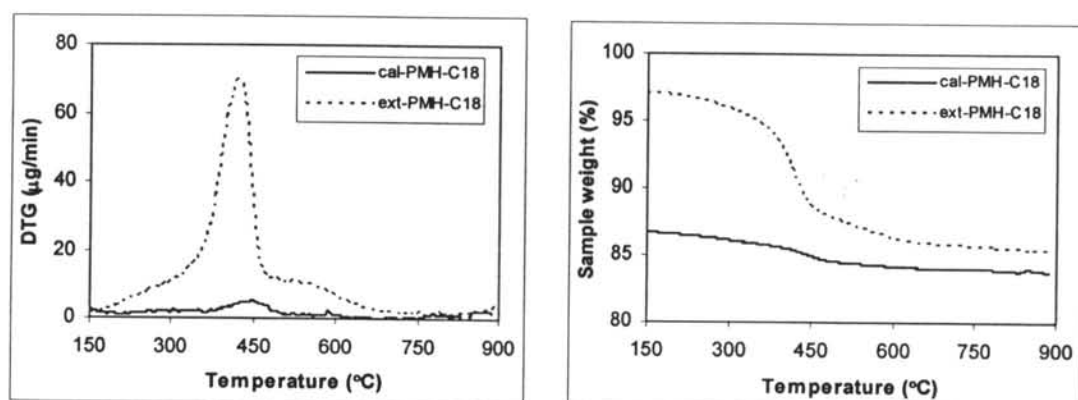
(C)

Figure 4.11 TG-DTA curves of the calcined and extracted PMH (A) PMH–C$_{12}$ (B) PMH–C$_{16}$ (C) PMH–C$_{18}$.

(A)

(B)

(C)

Figure 4.12 TG-DTA curves of the calcined and extracted PBH (A) PBH–C_{12} (B) PBH–C_{16} (C) PBH–C_{18}.

Table 4.5 Comparison of the % organic residue of PMH and PBH between calcination and solvent extraction

Sample	% organic residue	
	Calcination	Solvent extraction
PMH-C$_{12}$	2.4	10.1
PMH-C$_{16}$	1.9	9.0
PMH-C$_{18}$	2.4	11.3
PBH-C$_{12}$	1.9	7.7
PBH-C$_{16}$	2.2	8.2
PBH-C$_{18}$	1.6	8.1

4.5 CONCLUSIONS

Porous clay heterostructures (PCH) were successfully synthesized by the surfactant-directed assembly of mesostructured silica within clay layers. Two types of clay (montmorillonite and bentonite) were used in this synthesis to obtain montmorillonite PCH (designated PMH) and bentonite PCH (designated PBH). In the last step of the synthesis, the surfactants (templates) are removed either by calcination or by solvent extraction. The surfactant residual of the calcined PCH is less than 3% while the extracted PCH is about 8-12%. The shapes of the N$_2$ adroption-desorption isotherms of calcined and extracted-PCH are very similar which belong to a type IV BET isotherm and show a type B hysteresis loop. Due to the increase in local heating, calcination can result in slightly structural collapses and give lower porosities. This is also evidenced by the larger hysteresis loop appearing in the adsorption-desorption isotherm. The calcined and extracted PCH have a BET surface area in the range 400-700 m^2/g and the corresponding pore volumes were in range 0.3-0.5 cm^3/g. The pore sizes which analyzed by BJH method were 1.7-3.9 nm. The framework pore sizes were in the supermicropore to small mesopore range.

4.6 ACKNOWLEDGEMENTS

4.7 REFERENCES

[1]   Galarneau, A., Barodawalla, A., and Pinnavaia, T.J. Nature 374 (1995) 529.

[2]   Polverejan, M., Pauly, T.R., and Pinnavaia, T.J. Chem. Mater. 12 (2000) 2698.

[3]   Mercier, L., and Pinnavaia, T.J. Micropor. Mesopor. Mater. 20 (1998) 101.

[4]   Polverejan, M., Liu, Y., and Pinnavaia, T.J. Chem. Mater. 14 (2002) 2283.

[5]   Ahenach, J., Cool, P., and Vansant, E.F. Phys. Chem. Chem. Phys. 2 (2000) 5750.

[6]   Benjelloun, M., Cool, P., Linssen, T., and Vansant, E.F. Micropor. Mesopor. Mater. 49 (2001) 83.

[7]   Wei, L., Tang, T., and Huang, B. Micropor. Mesopor. Mater. 67 (2004) 175.

[8]   Zhou, C., Li, X., Ge, Z., Li, Q., and Tong, D. Catalysis Today 93-95 (2004) 607.

[9]   Nakatsuji, M., Ishii, R., Wang, Z., and Ooi, K., J. Colloid and Interface Science 272 (2004) 158.

[10]   Zhu, H.Y., Ding, Z., Lu, C.Q., and Lu, G.Q. Applied Clay Science 20 (2002) 165.

[11]   Pires, J., Araujo, A.C., Carvalho, A.P., Pinto, M.L., Gonzalez-Calbet, J.M., and Ramirez-Castellanos, J. Micropor. Mesopor. Mater. 73 (2004) 175.

[12]   Gregg, S.J., and Sing, K.S.W., Adsorption, Surface Area and Porosity (second edition), Academic Press, London, (1982) p.116.

[13]   Stein, A., Melde, B.J., and Schroden, R.C., Adv. Mater. 12 (2000) 1430.